Biochemical and Biophysical Research Communications 441 (2013) 544–549

Contents lists available at ScienceDirect

Biochemical and Biophysical Research Communications

journal homepage: www.elsevier.com/locate/ybbrc

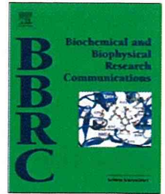

Treatment with 17-allylamino-17-demethoxygeldanamycin ameliorated symptoms of Bartter syndrome type IV caused by mutated *Bsnd* in mice

Naohiro Nomura [a], Kazusaku Kamiya [b], Katsuhisa Ikeda [b], Naofumi Yui [a], Motoko Chiga [a], Eisei Sohara [a], Tatemitu Rai [a], Sei Sakaki [a], Shinich Uchida [a,*]

[a] Department of Nephrology, Graduate School of Medical and Dental Sciences, Tokyo Medical and Dental University, 1-5-45 Yushima, Bunkyo-ku, Tokyo 113-8519, Japan
[b] Department of Otorhinolaryngology, Juntendo University Faculty of Medicine, 2-1-1 Hongo, Bunkyo-ku, Tokyo 113-8421, Japan

ARTICLE INFO

Article history:
Received 19 October 2013
Available online 1 November 2013

Keywords:
Bartter syndrome
Barttin
ClC-K
17-AAG
Sensorineural hearing impairment

ABSTRACT

Mutations of *BSND*, which encodes barttin, cause Bartter syndrome type IV. This disease is characterized by salt and fluid loss, hypokalemia, metabolic alkalosis, and sensorineural hearing impairment. Barttin is the β-subunit of the ClC-K chloride channel, which recruits it to the plasma membranes, and the ClC-K/barttin complex contributes to transepithelial chloride transport in the kidney and inner ear. The retention of mutant forms of barttin in the endoplasmic reticulum (ER) is etiologically linked to Bartter syndrome type IV. Here, we report that treatment with 17-allylamino-17-demethoxygeldanamycin (17-AAG), an Hsp90 inhibitor, enhanced the plasma membrane expression of mutant barttins (R8L and G47R) in Madin–Darby canine kidney cells. Administration of 17-AAG to $Bsnd^{R8L/R8L}$ knock-in mice elevated the plasma membrane expression of R8L in the kidney and inner ear, thereby mitigating hypokalemia, metabolic alkalosis, and hearing loss. These results suggest that drugs that rescue ER-retained mutant barttin may be useful for treating patients with Bartter syndrome type IV.

© 2013 Elsevier Inc. All rights reserved.

1. Introduction

Mutations of *BSND* that encode barttin cause Bartter syndrome type IV [1]. This disease is characterized by salt and fluid loss, hypokalemia, metabolic alkalosis, and sensorineural hearing impairment. Patients with Bartter syndrome are typically treated with potassium-sparing diuretics such as spironolactone or amiloride, angiotensin inhibitors, and potassium supplementation and frequently treated with nonsteroidal anti-inflammatory drugs to suppress the elevation of renal prostaglandin E2. However, these treatments only partially ameliorate Bartter syndrome symptoms. Sensorineural hearing impairment accompanies renal symptoms; however, no treatment is available for this impairment.

Barttin is the β-subunit of ClC-K chloride channels that are expressed in the distal renal tubules and inner ear [2]. Barttin is coexpressed with ClC-K1 in apical and basolateral membranes of the thin ascending limb of Henle's loop [3,4] and with ClC-K2 in the basolateral plasma membranes of nephron segments from the thick ascending limb of Henle's loop to intercalated cells in collecting ducts [5–7]. Constitutive barttin knockout mice die a few days after birth because of severe dehydration [8]. Moreover, barttin hypomorphic mice suffer from severe polyuria, hypokalemia, and metabolic alkalosis [9]. These findings indicate that ClC-K/barttin plays a crucial role in transepithelial chloride transport in the kidney.

Barttin colocalizes with ClC-K1 and ClC-K2 in the basolateral membrane of marginal cells of the stria vascularis and vestibular dark cells [2]. Mechanical vibration is enhanced and converted to electrical signals through outer and inner hair cells in the organ of Corti. To allow a depolarizing influx of potassium ions through apical mechanosensitive cation channels of hair cells, the endolymph that fills the cavity of the scala media is high in K^+ and has a positive potential [10,11]. These conditions are generated by the stria vascularis, which comprises a multilayered epithelium [11,12]. Inner ear-specific barttin knockout mice show a significant decrease of endocochlear potential (EP) and are congenitally deaf [8], indicating that barttin/ClC-K is required to generate EP.

Patients with Bartter syndrome type IV harbor different *BSND* mutations [1,13–20]. The R8L missense mutant barttin does not activate the ClC-K chloride channel currents when introduced into *Xenopus laevis* oocytes, and R8L barttin and C1C-K are not expressed on the plasma membrane [2,21]. We showed that the R8L barttin stably expressed in Madin–Darby canine kidney (MDCK) cells was trapped in the endoplasmic reticulum (ER) and did not reach the plasma membrane [22]. Recently, we confirmed this phenotype in the kidneys of $Bsnd^{R8L/R8L}$ knock-in mice (R8L knock-in mice) [9].

* Corresponding author. Fax: +81 3 5803 5215.
E-mail address: suchida.kid@tmd.ac.jp (S. Uchida).

0006-291X/$ - see front matter © 2013 Elsevier Inc. All rights reserved.
http://dx.doi.org/10.1016/j.bbrc.2013.10.129

Certain pathogenic proteins are misfolded and are retained in the ER, including the cystic fibrosis transmembrane conductance regulator (CFTR) [23–26], aquaporin 2 (AQP2) [27,28], V2 vasopressin receptor [29,30], podocin [31], and Tamm–Horsfall Protein (THP) [32]. Attempts have been made to rescue these ER-trapped mutant proteins. For example, the Hsp90 inhibitor 17-allylamino-17-demethoxygeldanamycin (17-AAG) increases cell-surface expression of AQP2-T125 M and partially corrects nephrogenic diabetes insipidus phenotype in $AQP2^{T126M/-}$ mice [28]. Moreover, 17-AAG increases the stability of mutant pendrin by inhibiting its ubiquitin-mediated degradation [33].

In the present study, we investigated the effect of 17-AAG treatment on mislocalized R8L barttin in MDCK cells and in R8L knock-in mice. We found that 17-AAG increased the expression of R8L barttin on the plasma membrane and partially ameliorated the phenotypes of Bartter syndrome type IV, including hearing loss.

2. Material and methods

2.1. Cell culture and analysis of cell-surface expression of barttin

We used MDCK cells stably expressing wild-type (WT) and R8L mutant barttin, which are described in our previous study [22]. G47R mutant barttin stably expressing MDCK cells were generated with site-directed mutagenesis and G418 selection as previously described [22]. Cell-surface proteins were harvested using a published side-specific biotinylation technique [34]. MDCK cells were incubated in the wells of 6-well TransWell filters (Corning) for at least 3 days to form confluent monolayers and were then incubated with 17-AAG (LC Laboratories), curcumin (Sigma–Aldrich), trimethylamine oxide (TMAO) (Sigma–Aldrich), or DMSO (0.15%) as control for 2 h before biotinylation. Cells were biotinylated using EZ-Link Sulfo-NHS-SS-biotin (Thermo Scientific) for 30 min. After quenching the remaining biotin with 50 mM NH_4Cl, cells were lysed with lysis buffer (150 mM NaCl, 20 mM Tris–HCl, 5 mM EDTA, and 1% Trion-X-100). Biotinylated proteins were bound to NeutrAvidin resin (Thermo Scientific), eluted using sodium dodecyl sulfate polyacrylamide gel electrophoresis (SDS–PAGE) buffer containing 50 mM dithiothreitol at 60 °C for 20 min and then subjected to immunoblotting. Blots were incubated with an anti-barttin antibody diluted to 1:200 with 5% skim milk in Tris-buffered saline with tween (TBST) [9]. Immunofluorescence (IF) detection of barttin in MDCK cells grown on filters was performed as follows. The cells were fixed with 3% paraformaldehyde (PFA) for 15 min, permeabilized with 0.1% Triton X-100 in PBS for 10 min, blocked in 1% bovine serum albumin (BSA) in phosphate buffered saline (PBS) for 30 min, and then incubated with the anti-barttin antibody (1:200 dilution with 1% BSA in PBS) for 2 h at room temperature. Alexa-Fluor®-labeled secondary antibodies (Life Technologies) were used to detect the barttin-primary antibody complexes. IF images were observed using an LSM510 Meta fluorescence microscope (Carl Zeiss).

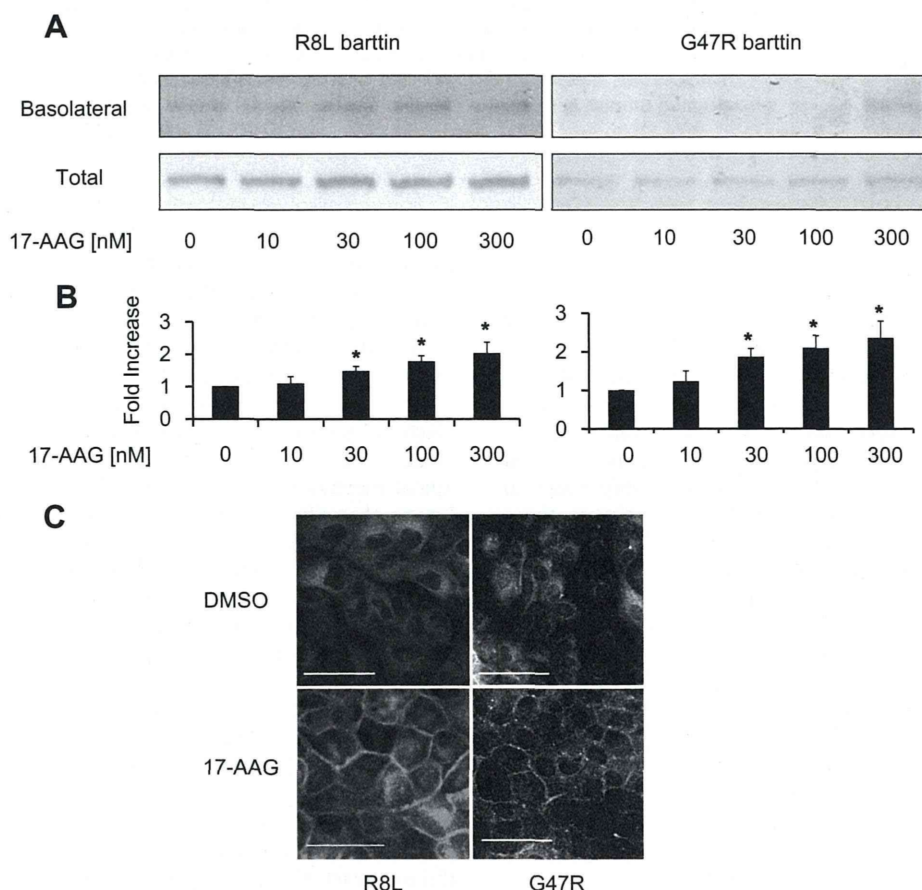

Fig. 1. Effect of 17-allylamino-17-demethoxygeldanamycin (17-AAG) on cell-surface expression of R8L and G47R mutant barttins R8L and G47R were stably expressed in Madin–Darby canine kidney (MDCK) cells. The cells were incubated with 17-AAG 2 h before biotin labeling and IF analysis. (A) Expression of R8L and G47R in basolateral plasma membranes increased after treatment with >30 nM 17-AAG. (B) Densitometric analyses of the data shown in Fig. 1A. $N = 4$ (R8L), $N = 3$ (G47R), $^*p < 0.05$. (C) Immunofluorescence analysis of R8L and G47R showing increased expression on the plasma membrane after treatment with 17-AAG (300 nM). At least three independent experiments yielded similar results. Scale bars = 50 μM.

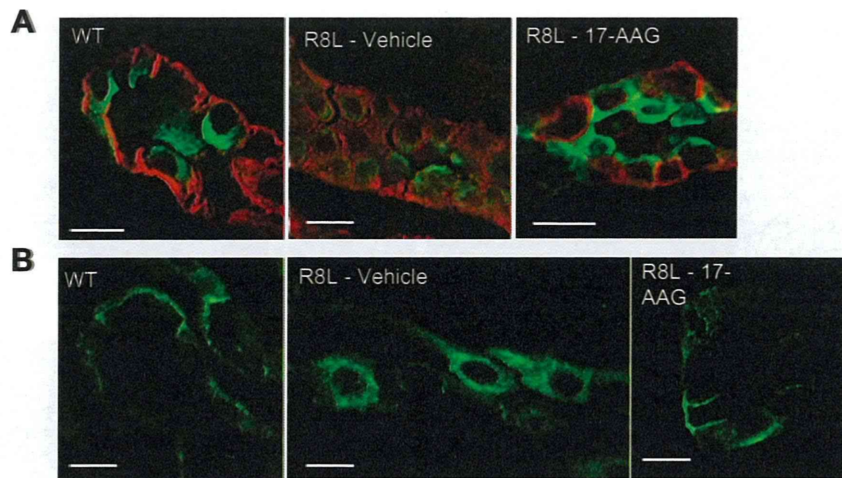

Fig. 2. Representative images of R8L barttin and ClC-K in the kidney of an R8L knock-in mice after 17-allylamino-17-demethoxygeldanamycin (17-AAG) treatment 17-AAG (25 mg/kg) or dimethyl sulfoxide (DMSO; vehicle control) was intraperitoneally administered. (A) 17-AAG restored the plasma membrane localization of R8L barttin (red) in connecting tubules. Apical green staining identifies AQP2. (B) Localization of ClC-K in intercalated cells in the cortical connecting duct was corrected by 17-AAG treatment in R8L knock-in mice. WT: wild-type mice, R8L: R8L knock-in mice. Scale bars = 10 μm. (For interpretation of the references to colour in this figure legend, the reader is referred to the web version of this article.)

Table 1
Analysis of blood samples obtained from R8L knock-in mice before and after17-allylamino-17-demethoxygeldanamycin (17-AAG) treatment.

	DMSO + Low NaCl diet (*N* = 10)		17-AAG + Low NaCl diet (*N* = 9)	
	Before treatment (regular)	After treatment (low NaCl)	Before treatment (regular)	After treatment (low NaCl)
Na (mEq/L)	147 ± 0	143 ± 1*	146 ± 1	142 ± 1*
K (mEq/L)	4.5 ± 0.2	3.9 ± 0.2*	4.7 ± 0.1	4.5 ± 0.1†
Cl (mEq/L)	111 ± 1	106 ± 1*	111 ± 1	108 ± 1*
pH	7.294 ± 0.015	7.345 ± 0.016*	7.285 ± 0.012	7.321 ± 0.018
HCO_3^- (mEq/L)	22.8 ± 0.4	25.6 ± 0.6*	22.6 ± 0.4	24.1 ± 0.8

The knock-in mice were injected with 17-allylamino-17-demethoxygeldanamycin (17-AAG) (25 mg/kg) or dimethyl sulfoxide (DMSO; vehicle control) daily for 7 days. The mice were fed a low salt diet during treatment. Plasma HCO_3^- levels and pH of DMSO-treated mice fed a low salt diet increased. However, the increase of plasma HCO_3^- and pH in 17-AAG-treated mice was not significant. DMSO-treated mice fed a low salt diet were hypokalemic; however, 17-AAG-treated mice were not.

* $p < 0.05$ vs. Pre.

† $p < 0.05$ vs. DMSO. Na, sodium; K, potassium; Cl, chloride; HCO_3^-, bicarbonate.

2.2. Immunofluorescent analysis of mouse tissues

The Animal Care and Use Committee of Tokyo Medical and Dental University approved the experiments conducted using animals. Mice were intraperitoneally administered 17-AAG (25 mg/kg) 2 h before tissue preparation. 17-AAG was dissolved in 50% DMSO, and the same volume of 50% DMSO was used as a vehicle control. Tissues were prepared as described previously [35]. Mice were deeply anesthetized with ether, and tissues were harvested and fixed with 4% PFA in PBS by perfusion through the left ventricle. The kidneys were removed and placed in the fixative. To prepare inner ear specimens, the temporal bones were removed and placed in the fixative. Small openings were made at the round and oval windows and at the apex of the cochlea, and the perilymphatic space was then gently perfused with fixative. After 1 h, the right temporal bones were decalcified by immersion in 5% ethylenediaminetetraacetic acid with stirring at 4 °C for approximately 7 days. Kidney and right inner-ear specimens were soaked for several hours in 20% sucrose in PBS, embedded in Tissue-Tek OCT compound (Sakura Finetechvical Co., Ltd.), and snap frozen. For whole-mount staining of the stria vascularis, fixed left-inner ears were microdissected, and the isolated stria vascularis was soaked in fixative. The whole-mount samples were treated with 0.5% Triton X-100 in PBS for 30 min. Frozen sections and whole-mount samples were blocked using 1% BSA in PBS and incubated with primary antibodies as follows: anti-barttin (diluted 1:200 with 0.1% BSA in PBS) [9] and anti-ClC-K (diluted 1:100) [36]. The secondary antibodies were conjugated to Alexa-Fluor® (diluted 1:200). Samples were mounted using VECTASHIELD® with DAPI (Vector Laboratories).

2.3. Analysis of blood

Blood was collected from the submandibular vein after administering light anesthesia with ether. Blood data was determined using an i-STAT® analyzer (Fuso, Osaka, Japan). Baseline blood data were acquired from mice fed a normal diet (0.4% NaCl). The mice were then fed a low salt diet (0.01% NaCl) that induces hypokalemia and metabolic alkalosis in R8L barttin knock-in mice. We administered intraperitoneal injections of 25 mg/kg 17-AAG once daily for 7 days. Blood samples were collected after the treatment period. All nutrients were obtained from the Oriental Yeast Co., Ltd., (Tokyo, Japan).

2.4. Auditory brainstem response (ABR)

ABR recording was performed as previously described [35]. Mice were anesthetized using pentobarbital before placing stainless steel needle electrodes dorsolaterally to the ears. Waveforms of 512 stimuli (9 Hz) were averaged, and the visual detection threshold was determined using varying sound pressure levels. Baseline hearing thresholds were recorded first. After 2 h of

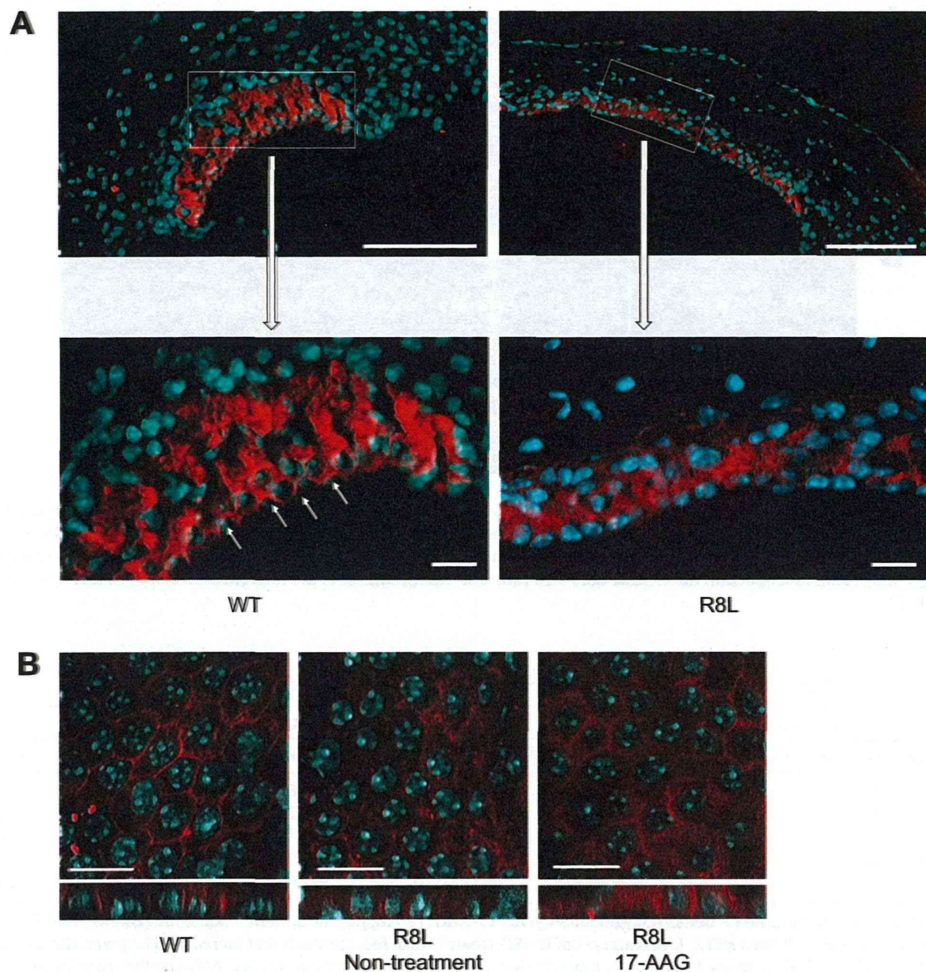

Fig. 3. Representative images of barttin in the stria vascularis. (A) Representative images of barttin in frozen sections of the stria vascularis. Wild-type (WT) barttin appeared to be present on the lateral walls of marginal cells (arrows), whereas R8L expression on the plasma membrane was not clear. Blue indicates nuclear (DAPI) staining. Scale bars = 100 μm in upper panels, 20 μm in lower panels. (B) Representative images of barttin (red) in whole mounts of the stria vascularis. Blue indicates nuclear (DAPI) staining. Scale bars = 20 μm. Lower panels show z-stacks of upper panels. Wild-type (WT) barttin was observed on the lateral walls of marginal cells (left panel), whereas R8L expression on the plasma membrane was not clear (middle panel). 17-AAG treatment partially restored the plasma membrane expression of R8L (right panel). (For interpretation of the references to colour in this figure legend, the reader is referred to the web version of this article.)

Table 2
Hearing thresholds (dB) of wild-type (WT) and R8L knock-in mice assessed using auditory brainstem response (ABR).

Frequency		3-Week-old mice	5-Week-old mice	10-Week-old mice
8000 Hz	WT	16.0 ± 2.0	19.9 ± 1.7	21.8 ± 1.4
	R8L	36.0 ± 2.8*	54.9 ± 2.9*†	70.4 ± 3.3*†§
20,000 Hz	WT	6.7 ± 2.3	14.1 ± 2.8	13.4 ± 0.0
	R8L	42.6 ± 5.5*	50.9 ± 2.0*	63.4 ± 2.9*†§

The numbers of mice are shown in Fig. 4A.
* $p < 0.05$ vs. WT.
† $p < 0.05$, 3-week-old mice.
§ $p < 0.05$, 5-week-old mice.

recovery from anesthesia, 17-AAG (25 mg/kg) or vehicle (equal volume of 50% DMSO) was intraperitoneally injected and hearing thresholds were determined again.

2.5. Statistical methods

All values are expressed as the mean ± standard error of the mean (SE). Statistical analyses of the effects of treatment were performed using a paired *t*-test. Other statistical analyses were performed using an unpaired *t*-test. *p*-Values <0.05 were considered statistically significant.

3. Results

3.1. Cell-surface expression of mutant barttins by MDCK cells is increased by treatment with 17-AAG

Analysis of MDCK cells stably expressing human R8L and G47R barttins showed that barttin localization was primarily intracellular (Fig. 1). We next tested whether agents that rescue ER-trapped membrane proteins (17-AAG, curcumin, and TMAO) [23,25,26,28,33] were effective in relocalizing the mutant barttins. IF and site-specific biotin labeling revealed that these agents effectively increased the basolateral plasma membrane expression of the mutant proteins (Fig. 1 and Fig. S1). Moreover, the basolateral expression of WT barttin did not increase in response to 17-AAG (Fig. S2). We also assessed the effects of 17-AAG on barttin mutants G10S, I12T, Q32X; however, G10S and I12T mutant barttin were expressed on the plasma membrane before the treatment [17,22,37], and the low level of Q32X barttin expression did not permit the acquisition of meaningful data.

3.2. Partial rescue of renal phenotypes of R8L knock-in mice

We previously showed that R8L and ClC-K expression in the basolateral membrane is significantly decreased in the renal

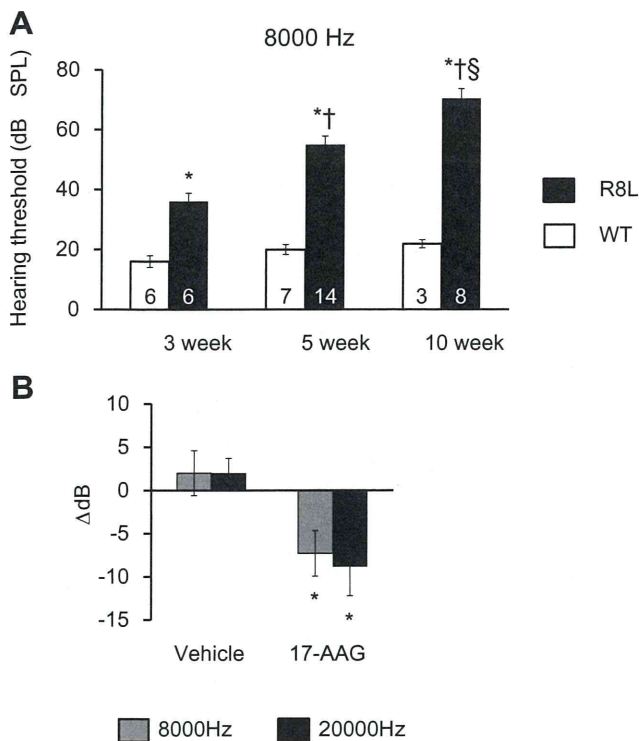

Fig. 4. Hearing impairment in R8L knock-in mice and its amelioration with 17-AAG treatment (A) Hearing thresholds at 8000 Hz in wild-type (WT) and R8L knock-in mice measured using auditory brainstem response (ABR). Numbers of mice are shown on the columns. $^{*}p < 0.05$ vs. WT, $^{\dagger}p < 0.05$ vs. 3-week-old mice, $^{\S}p < 0.05$ vs. 5-week-old mice. (B) Variation of hearing thresholds before and after treatment. 17-allylamino-17-demethoxygeldanamycin (17-AAG): $N = 13$; vehicle: $N = 10$. $^{*}p < 0.05$ vs. vehicle.

tubules of R8L knock-in mice [9]. IF analysis of the R8L mutants shows that 17-AAG restored the basolateral localization of barttin in the connecting tubules (Fig. 2) and corrected the intracellular localization of ClC-K in the intercalated cells of cortical collecting ducts (Fig. 2).

The R8L knock-in mice suffered from metabolic alkalosis and hypokalemia when fed a low-salt diet [9]. We confirmed our previous findings in the vehicle-treated R8L knock-in mice (Table 1). However, administration of 17-AAG for one week corrected the low salt-induced metabolic alkalosis and ameliorated hypokalemia (Table 1). In wild-type mice, administration of 17-AAG did not significantly affect these parameters (Table S1).

3.3. *Partial rescue of sensorineural hearing impairment of R8L knock-in mice*

IF analysis revealed that R8L was present in the stria vascularis (Fig. 3A). In higher magnification (lower panels), wild-type barttin appeared to be localized on the lateral walls of marginal cells (arrows), whereas R8L expression on the plasma membrane was not clear. However, it was difficult to assess from this view whether localization of R8L to the plasma membrane was impaired because marginal and intermediate cells are extensively interdigitated. Therefore, we analyzed whole-mount samples (Fig. 3B) and confirmed the finding shown in Fig. 3A. Furthermore, we could observe that 17-AAG treatment partially restored the plasma membrane expression of R8L (Fig. 3B, right panel).

We evaluated hearing impairment using ABR. R8L knock-in mice lost hearing at 8 and 20 kHz compared with control WT littermates at 3-, 6-, and 10-weeks of age (Table 2, Fig. 4A). Although 17-AAG treatment did not affect the hearing thresholds of WT mice (Table S2), it slightly, but significantly, improved the hearing thresholds of R8L knock-in mice (Fig. 4B). DMSO treatment did not affect hearing thresholds.

4. Discussion

We previously described the renal phenotypes of R8L barttin knock-in mice [9]. Bartter-like phenotypes (loss of salt from the kidney, hypokalemia, and metabolic alkalosis) were only observed when these mice were fed a low salt diet. In contrast to the renal phenotypes, we found here that the hearing of R8L knock-in mice was significantly impaired under normal conditions. Because ABR analysis generated semi-quantitative data indicating impaired function of ClC-K/R8L barttin in vivo, we used this parameter to assess the reversal of symptoms by administering 17-AAG to R8L knock-in mice. We observed significant improvement in the hearing threshold as well as the increased expression of barttin at the plasma membrane. Metabolic alkalosis and hypokalemia were also ameliorated by 17-AAG treatment, which increased the plasma membrane expression of R8L barttin in renal tubules. 17-AAG, a semisynthetic chemical analog of the natural product geldanamycin, inhibits Hsp90 function [38]. Hsp90 participates in a diverse range of cellular processes, including chaperoning of newly synthesized proteins, stress responses, signal transduction, and transcriptional regulation [39]. We chose 17-AAG for the present study because 17-AAG is effective at low concentrations in vitro and has been used in other mouse models of human diseases [28] as well as for treating patients with cancer [40,41]. We previously demonstrated that decreased transepithelial chloride transport and plasma membrane localization of barttin significantly correlate in the thin limb of Henle's loop of R8L knock-in mice, providing compelling evidence that impaired plasma membrane localization of R8L barttin accounts for pathogenesis. We demonstrate that 17-AAG was effective for rerouting barttin to the plasma membrane of MDCK cells expressing R8L and G47R barttin. Therefore, 17-AAG may be useful for treating patients with Bartter syndrome type IV who harbor other *BSND* missense mutations.

The mechanism underlying the ability of 17-AAG to rescue mutant barttins is unknown. ER-retained mutant barttins may be misfolded and are restored to their native conformations by 17-AAG. This assumption is supported by findings that TMAO and curcumin were also effective in increasing barttin expression at the plasma membrane (Fig. S1). However, it was difficult to confirm this hypothesis from these experiments because the maturation of barttin (an unglycosylated protein) cannot be monitored by its glycosylation. Findings related to those reported here demonstrate that the treatment of human cell lines with 17-AAG facilitates the folding of pendrin through heat shock transcription factor 1-dependent induction of molecular chaperones [33], suggesting that the same mechanism mediates the effects of 17-AAG on R8L and G47R barttin. Restoration from the misfolding by 17-AAG might not only correct the mislocalization of R8L but also decrease ER-associated degradation of R8L, both of which might be involved in the increased plasma membrane expression of R8L by 17-AAG.

In conclusion, we demonstrated that the hearing of patients with Bartter syndrome type IV may be restored by treatment with drugs such as 17-AAG. Further research is required to discover more effective drugs that correct the aberrant intracellular localization of misfolded membrane proteins.

Acknowledgments

We thank Dr. T. Jentsch, Leibniz-Institut für Molekulare Pharmakologie and Max-Delbrück-Centrum für Molekulare Medizin, for generously providing anti-ClC-K antibody. This study was supported in part by Grants-in-Aid for Scientific Research (S) from the

Japan Society for the Promotion of Science, Health Labor Science Research Grant from the Ministry of Health Labor and Welfare, Salt Science Research Foundation (Nos. 1026, 1228), Banyu Foundation Research Grant, and Takeda Science Foundation.

Appendix A. Supplementary data

Supplementary data associated with this article can be found, in the online version, at http://dx.doi.org/10.1016/j.bbrc.2013.10.129.

References

[1] R. Birkenhäger, E. Otto, M. Schürmann, M. Vollmer, E. Ruf, I. Maier-Lutz, F. Beekmann, A. Fekete, H. Omran, D. Feldmann, D. Milford, N. Jeck, M. Konrad, D. Landau, N. Knoers, C. Antignac, R. Sudbrak, A. Kispert, F. Hildebrandt, Mutation of BSND causes Bartter syndrome with sensorineural deafness and kidney failure, Nat. Genet. 29 (2001) 310–314.

[2] R. Estévez, T. Boettger, V. Stein, R. Birkenhäger, E. Otto, F. Hildebrandt, T. Jentsch, Barttin is a Cl^- channel beta-subunit crucial for renal Cl^- reabsorption and inner ear K^+ secretion, Nature 414 (2001) 558–561.

[3] S. Uchida, S. Sasaki, K. Nitta, K. Uchida, S. Horita, H. Nihei, F. Marumo, Localization and functional characterization of rat kidney-specific chloride channel, ClC-K1, J. Clin. Invest. 95 (1995) 104–113.

[4] S. Uchida, S. Sasaki, T. Furukawa, M. Hiraoka, T. Imai, Y. Hirata, F. Marumo, Molecular cloning of a chloride channel that is regulated by dehydration and expressed predominantly in kidney medulla, J. Biol. Chem. 268 (1993) 3821–3824.

[5] M. Yoshikawa, S. Uchida, A. Yamauchi, A. Miyai, Y. Tanaka, S. Sasaki, F. Marumo, Localization of rat CLC-K2 chloride channel mRNA in the kidney, Am. J. Physiol. 276 (1999) F552–F558.

[6] K. Kobayashi, S. Uchida, S. Mizutani, S. Sasaki, F. Marumo, Intrarenal and cellular localization of CLC-K2 protein in the mouse kidney, J. Am. Soc. Nephrol. 12 (2001) 1327–1334.

[7] S. Adachi, S. Uchida, H. Ito, M. Hata, M. Hiroe, F. Marumo, S. Sasaki, Two isoforms of a chloride channel predominantly expressed in thick ascending limb of Henle's loop and collecting ducts of rat kidney, J. Biol. Chem. 269 (1994) 17677–17683.

[8] G. Rickheit, H. Maier, N. Strenzke, C. Andreescu, C. De Zeeuw, A. Muenscher, A. Zdebik, T. Jentsch, Endocochlear potential depends on Cl^- channels: mechanism underlying deafness in Bartter syndrome IV, EMBO J. 27 (2008) 2907–2917.

[9] N. Nomura, M. Tajima, N. Sugawara, T. Morimoto, Y. Kondo, M. Ohno, K. Uchida, K. Mutig, S. Bachmann, M. Soleimani, E. Ohta, A. Ohta, E. Sohara, T. Okado, T. Rai, T.J. Jentsch, S. Sasaki, S. Uchida, Generation and analyses of R8L barttin knockin mouse, Am. J. Physiol. Renal Physiol. 301 (2011) F297–F307.

[10] H. Hibino, Y. Kurachi, Molecular and physiological bases of the K^+ circulation in the mammalian inner ear, Physiology (Bethesda) 21 (2006) 336–345.

[11] P. Wangemann, Supporting sensory transduction: cochlear fluid homeostasis and the endocochlear potential, J. Physiol. 576 (2006) 11–21.

[12] F. Nin, H. Hibino, K. Doi, T. Suzuki, Y. Hisa, Y. Kurachi, The endocochlear potential depends on two K^+ diffusion potentials and an electrical barrier in the stria vascularis of the inner ear, Proc. Natl. Acad. Sci. USA 105 (2008) 1751–1756.

[13] Z. Bircan, F. Harputluoglu, N. Jeck, Deletion of exons 2–4 in the BSND gene causes severe antenatal Bartter syndrome, Pediatr. Nephrol. 24 (2009) 841–844.

[14] F. Ozlu, H. Yapicioğlu, M. Satar, N. Narli, K. Ozcan, M. Buyukcelik, M. Konrad, O. Demirhan, Barttin mutations in antenatal Bartter syndrome with sensorineural deafness, Pediatr. Nephrol. 21 (2006) 1056–1057.

[15] N. Miyamura, K. Matsumoto, T. Taguchi, H. Tokunaga, T. Nishikawa, K. Nishida, T. Toyonaga, M. Sakakida, E. Araki, Atypical Bartter syndrome with sensorineural deafness with G47R mutation of the beta-subunit for ClC-Ka and ClC-Kb chloride channels, barttin, J. Clin. Endocrinol. Metab. 88 (2003) 781–786.

[16] V. García-Nieto, C. Flores, M. Luis-Yanes, E. Gallego, J. Villar, F. Claverie-Martín, Mutation G47R in the BSND gene causes Bartter syndrome with deafness in two Spanish families, Pediatr. Nephrol. 21 (2006) 643–648.

[17] S. Riazuddin, S. Anwar, M. Fischer, Z. Ahmed, S. Khan, A. Janssen, A. Zafar, U. Scholl, T. Husnain, I. Belyantseva, P. Friedman, T. Friedman, C. Fahlke, Molecular basis of DFNB73: mutations of BSND can cause nonsyndromic deafness or Bartter syndrome, Am. J. Hum. Genet. 85 (2009) 273–280.

[18] S. Kitanaka, U. Sato, K. Maruyama, T. Igarashi, A compound heterozygous mutation in the BSND gene detected in Bartter syndrome type IV, Pediatr. Nephrol. 21 (2006) 190–193.

[19] M. Zaffanello, A. Taranta, A. Palma, A. Bettinelli, G. Marseglia, F. Emma, Type IV Bartter syndrome: report of two new cases, Pediatr. Nephrol. 21 (2006) 766–770.

[20] S. Brum, J. Rueff, J. Santos, J. Calado, Unusual adult-onset manifestation of an attenuated Bartter's syndrome type IV renal phenotype caused by a mutation in BSND, Nephrol. Dial. Transplant. 22 (2007) 288–289.

[21] S. Waldegger, N. Jeck, P. Barth, M. Peters, H. Vitzthum, K. Wolf, A. Kurtz, M. Konrad, H. Seyberth, Barttin increases surface expression and changes current properties of ClC-K channels, Pflugers Arch. 444 (2002) 411–418.

[22] A. Hayama, T. Rai, S. Sasaki, S. Uchida, Molecular mechanisms of Bartter syndrome caused by mutations in the BSND gene, Histochem. Cell Biol. 119 (2003) 485–493.

[23] H. Fischer, N. Fukuda, P. Barbry, B. Illek, C. Sartori, M. Matthay, Partial restoration of defective chloride conductance in DeltaF508 CF mice by trimethylamine oxide, Am. J. Physiol. Lung Cell. Mol. Physiol. 281 (2001) L52–L57.

[24] S. Sato, C.L. Ward, M.E. Krouse, J.J. Wine, R.R. Kopito, Glycerol reverses the misfolding phenotype of the most common cystic fibrosis mutation, J. Biol. Chem. 271 (1996) 635–638.

[25] M. Egan, M. Pearson, S. Weiner, V. Rajendran, D. Rubin, J. Glöckner-Pagel, S. Canny, K. Du, G. Lukacs, M. Caplan, Curcumin, a major constituent of turmeric, corrects cystic fibrosis defects, Science 304 (2004) 600–602.

[26] C. Brown, L. Hong-Brown, J. Biwersi, A. Verkman, W. Welch, Chemical chaperones correct the mutant phenotype of the delta F508 cystic fibrosis transmembrane conductance regulator protein, Cell Stress Chaperones 1 (1996) 117–125.

[27] B.K. Tamarappoo, A.S. Verkman, Defective aquaporin-2 trafficking in nephrogenic diabetes insipidus and correction by chemical chaperones, J. Clin. Invest. 101 (1998) 2257–2267.

[28] B. Yang, D. Zhao, A. Verkman, Hsp90 inhibitor partially corrects nephrogenic diabetes insipidus in a conditional knock-in mouse model of aquaporin-2 mutation, FASEB J. 23 (2009) 503–512.

[29] J.P. Morello, A. Salahpour, A. Laperrière, V. Bernier, M.F. Arthus, M. Lonergan, U. Petäjä-Repo, S. Angers, D. Morin, D.G. Bichet, M. Bouvier, Pharmacological chaperones rescue cell-surface expression and function of misfolded V2 vasopressin receptor mutants, J. Clin. Invest. 105 (2000) 887–895.

[30] V. Bernier, J.P. Morello, A. Zarruk, N. Debrand, A. Salahpour, M. Lonergan, M.F. Arthus, A. Laperrière, R. Brouard, M. Bouvier, D.G. Bichet, Pharmacologic chaperones as a potential treatment for X-linked nephrogenic diabetes insipidus, J. Am. Soc. Nephrol. 17 (2006) 232–243.

[31] T. Ohashi, K. Uchida, S. Uchida, S. Sasaki, H. Nihei, Intracellular mislocalization of mutant podocin and correction by chemical chaperones, Histochem. Cell Biol. 119 (2003) 257–264.

[32] L. Ma, Y. Liu, T.M. El-Achkar, X.R. Wu, Molecular and cellular effects of Tamm-Horsfall protein mutations and their rescue by chemical chaperones, J. Biol. Chem. 287 (2012) 1290–1305.

[33] K. Lee, T.J. Hong, J.S. Hahn, Roles of 17-AAG-induced molecular chaperones and Rma1 E3 ubiquitin ligase in folding and degradation of pendrin, FEBS Lett. 586 (2012) 2535–2541.

[34] N. Yui, R. Okutsu, E. Sohara, T. Rai, A. Ohta, Y. Noda, S. Sasaki, S. Uchida, FAPP2 is required for aquaporin-2 apical sorting at trans-Golgi network in polarized MDCK cells, Am. J. Physiol. Cell Physiol. 297 (2009) C1389–C1396.

[35] K. Kamiya, Y. Fujinami, N. Hoya, Y. Okamoto, H. Kouike, R. Komatsuzaki, R. Kusano, S. Nakagawa, H. Satoh, M. Fujii, T. Matsunaga, Mesenchymal stem cell transplantation accelerates hearing recovery through the repair of injured cochlear fibrocytes, Am. J. Pathol. 171 (2007) 214–226.

[36] A. Vandewalle, F. Cluzeaud, M. Bens, S. Kieferle, K. Steinmeyer, T. Jentsch, Localization and induction by dehydration of ClC-K chloride channels in the rat kidney, Am. J. Physiol. 272 (1997) F678–F688.

[37] A. Janssen, U. Scholl, C. Domeyer, D. Nothmann, A. Leinenweber, C. Fahlke, Disease-causing dysfunctions of barttin in Bartter syndrome type IV, J. Am. Soc. Nephrol. 20 (2009) 145–153.

[38] S. Sharp, P. Workman, Inhibitors of the Hsp90 molecular chaperone: current status, Adv. Cancer Res. 95 (2006) 323–348.

[39] L. Pearl, C. Prodromou, P. Workman, The Hsp90 molecular chaperone: an open and shut case for treatment, Biochem. J. 410 (2008) 439–453.

[40] M.A. Dimopoulos, C.S. Mitsiades, K.C. Anderson, P.G. Richardson, Tanespimycin as antitumor therapy, Clin. Lymphoma Myeloma Leuk. 11 (2011) 17–22.

[41] U. Banerji, A. O'Donnell, M. Scurr, S. Pacey, S. Stapleton, Y. Asad, L. Simmons, A. Maloney, F. Raynaud, M. Campbell, M. Walton, S. Lakhani, S. Kaye, P. Workman, I. Judson, Phase I pharmacokinetic and pharmacodynamic study of 17-allylamino, 17-demethoxygeldanamycin in patients with advanced malignancies, J. Clin. Oncol. 23 (2005) 4152–4161.

遺伝性難聴への内耳細胞治療法開発

幹細胞ホーミング機構を応用した遺伝性難聴に対する内耳細胞治療法の開発

神谷　和作

要約：難聴の原因は多岐にわたるが，近年の遺伝子改変動物開発技術の向上や多種のモデル動物の開発により多くの病態メカニズムが解明に近づいている．全ての先天性疾患の中でも頻度の高い遺伝性難聴においては，難聴家系や突然変異難聴マウスの遺伝子解析によって多くの遺伝性難聴原因遺伝子が同定されている．しかし遺伝性難聴の根本的治療法は未だ開発されていない．特に哺乳類の有毛細胞は再生能力を持たないため多能性幹細胞移植による有毛細胞修復が近年試みられている．多能性幹細胞移植は薬物治療や遺伝子治療と異なり細胞導入後の病変部への侵入や増殖・分化による病態に応じた修復が期待できる．しかし特殊なリンパ液で充たされた内耳の構造的特徴から，聴力を温存しつつ標的部位に前駆細胞を到達させ分化させることは非常に難しい．動物実験においても幹細胞を内耳病変部にて適切に分化させ，機能を回復させた報告はいまだ少ない．近年有毛細胞以外にも蝸牛線維細胞などの機能異常が単独で難聴病態の引き金となることも明らかとなっており，多様な細胞種による治療戦略が求められている．多能性幹細胞の損傷部への組織誘導（ホーミング）機構や組織環境（ニッシェ，niche）による分化誘導を十分に解明し，これを応用すれば細胞治療は内耳組織の変性や遺伝子異常に対する永続的治療に有効となる可能性が高い．我々は遺伝性難聴モデルとしてのコネキシン26等の遺伝子改変動物を用い，骨髄間葉系幹細胞や人工多能性幹細胞（iPS細胞）等の多能性幹細胞の分化制御や組織誘導の促進によって効率の高い内耳細胞治療法の開発を進めてきた．

1. 遺伝性難聴

先天性難聴は1000出生に1人と先天性疾患のうちでも最も頻度の高い疾患の1つである．そのうち半数が遺伝性とされており，聴覚と言語発育の著しい障害を引き起こす極めて高度なQOLの低下をもたらす．特にコネキシン26（Cx26）をコードするGJB2遺伝子の変異は日本人の遺伝性難聴の20〜30％を占め，世界でも最も高頻度に出現する難聴原因遺伝子として知られている．

2. 内耳イオン輸送機構・K^+リサイクリングシステム

Cx26は他のコネキシン（Cx30等）とギャップジャンクションを構成し，内耳イオンの受動輸送体として重要な機能を担っている．これらはNa^+/K^+ATPase等の能動輸送体とともに蝸牛管を充たす内リンパ液（endolymph）のイオン組成を常に一定に保つことにより聴覚シグナルの機械的振動を神経シグナルに変換することを可能としている．内リンパ液は常に高K^+濃度（150 mM）と高電位（+80 mV）が維持されている．後者を蝸牛内リンパ電位（endocochlear potential：EP）と呼ぶ．内リンパ液に面している有毛細胞はEPがあるために音の振動から聴毛に存在する機械電気変換（mechanoelectrical transduction：MET）チャネルの開口によるイオン流入で有毛細胞が脱分極し，神経伝達物質を放出する．このEPを維持するために重要な役割を担っているのが有毛細胞を取り巻く蝸牛支持細胞，蝸牛線維細胞と血管条細胞であり，これらはコネキシンで構成されるギャップジャンクション，Na^+,K^+-ATPase，Na^+,K^+,$2Cl^-$共輸送体などによってイオン輸送を行い内リンパ液の高K^+状態を維持している(1, 2)．このイオン輸送システムはK^+リサイクリングシステムと呼ばれ，これが正常に機能しなければEPは低下し，たとえ有毛細胞機能が正常であってもイオン流入・脱分極は起こらず聴覚系神経の活動電位

キーワード：内耳幹細胞治療，内耳幹細胞ホーミング機構，骨髄間葉系幹細胞，蝸牛線維細胞，蝸牛有毛細胞
順天堂大学 医学部 耳鼻咽喉科学講座（〒113-8421 東京都文京区本郷2-1-1）
E-mail: kkamiya@juntendo.ac.jp 原稿受領日：2013年1月7日，依頼原稿
Title: Cell therapy for hereditary hearing loss with stem cell homing factors.　Author: Kazusaku Kamiya

は発生しない．

3. 内耳イオン輸送に障害を持つ遺伝性難聴モデル

1999年，Minowaらはヒト非症候性遺伝性難聴因子Brn-4の遺伝子欠損マウスの作成に成功しこの機能解析を報告した(3)．この研究ではヒト非症候性遺伝性難聴であるDFN3の原因が有毛細胞ではなくラセン靭帯の線維細胞の変性にあることが初めて証明された．さらに内リンパ電位の形成に線維細胞が不可欠であるという新しい内耳の生理学的知見を明らかにした．この線維細胞やコルチ器の支持細胞等に強く発現し内耳イオン輸送体として重要な機能を担うのがCx26だが，2003年，Cx26遺伝子で初の遺伝子改変難聴モデルが開発されると(4)，コルチ器の形成不全・機能障害など新たな分子病態が明らかとなった(5,6)．最近，内耳特異的Cx26遺伝子欠損マウスが新規に開発され，有用な難聴モデル動物としてさらなる新規分子病態が明らかとなっている．

4. 蝸牛線維細胞を標的とした内耳細胞治療法

我々は新規治療法開発を目的として，蝸牛線維細胞のみに限局的な損傷を持つ聴覚障害モデルを開発し(7,8)，半規管からの外リンパ液還流法による骨髄間葉系幹細胞移植により聴力回復を促進させることに初めて成功した(9)．それまで幹細胞導入によって蝸牛内の損傷を修復し聴力回復に成功した例はなく，蝸牛線維細胞をターゲットとした骨髄間葉系幹細胞の移植法は今後有効な治療手段となり得ることが証明された．この方法では細胞移植後の拒絶反応も少なく他家移植としての有用性も示され，遺伝子変異細胞を正常細胞に置換する方法としても十分応用可能であることが示された．

5. 人工多能性幹（iPS）細胞からの内耳前駆細胞の樹立

2010年，iPS細胞，ES細胞からin vitroで内耳有毛細胞を作製する画期的技術がOshimaらにより発表され，作製された細胞が音の振動を感知できる有毛細胞特有のMET機能を有することが明らかとなった(10)．2012年にはES細胞からの内耳前駆細胞の新規作製法と実験動物への応用が報告された(11)．これにより内耳有毛細胞を体外で人工的に増殖・分化させることが可能であることが示された．新規手法をもとに様々な分化状態の内耳前駆細胞を樹立し，内耳移植に最も適した分化度の細胞を選抜することが可能であると考えられる．これらの報告では，未分化細胞から外胚葉細胞，内耳前駆細胞へ，段階的に分化を進めており，これを応用して段階的に細胞の分離を行えば，難聴の原因となる全ての内耳構成細胞（有毛細胞，支持細胞，線維細胞，血管条細胞，ラセン神経節細胞）への分化能を持つ前駆細胞をin vitroにて作製し，標的細胞に応じた移植細胞を選抜することが可能となる．

我々の研究でもこの方法を応用することによりiPS細胞からMyosin7a発現とアクチン巨大繊毛を有する有毛細胞前駆細胞，コネキシン26発現細胞等が得られており，移植用幹細胞としての応用研究を進めている．

6. 新たな成体内耳幹細胞

最近，間葉系細胞への過剰ストレス負荷に耐性を持つ細胞から新たな多能性幹細胞が発見された(12)．同手法では遺伝子導入もなく安定的に増殖し間葉系幹細胞同様安全性が確保された幹細胞が得られると考えられる．我々はこの幹細胞樹立法を応用し成体内耳から初めて有毛細胞マーカーを発現する多能性幹細胞を樹立した．同細胞は一部に内耳有毛細胞のマーカーMyosin7aと共に細胞頂部に巨大繊毛様のアクチン重合を顕著に示す．この細胞は通常の間葉系幹細胞より増殖が二倍ほど遅く培養容器への強い接着を示すため，iPS細胞等から内耳前駆細胞への分化を誘導するためのフィーダー細胞としても適していた（未発表）．

7. 蝸牛標的組織への幹細胞の誘導

体外で内耳細胞を作製する技術は大きく進展しているが，作製された細胞を蝸牛組織へ直接的アプローチにて挿入することは蝸牛の構造上非常に困難である．Chenらの報告ではスナネズミのES細胞より分化誘導したラセン神経節細胞の前駆細胞を直接蝸牛軸へ注入し，神経細胞として機能させることに成功している(11)．蝸牛軸にガラス管等を挿入し細胞注入する導入方法は難易度が高く侵襲も高い．さらに齧歯類だけでも種間の解剖学的構造の差が大きく，人への臨床応用として安全性と有効性を確保することは困難なアプローチであると考えられる．感覚上皮である蝸牛有毛細胞とその支持細胞へのアプローチはさらに細胞構成が複雑なため困難が予想され，個体への生着と分化に成功した報告はいまだない．しかし適切な箇所に前駆細胞を挿入できる細胞誘導システムを開発すれば，低侵襲で安全かつ有効な技術が開発できると考えられる．筆者らは後半規管および外側半規管に小孔を開け，片側から微小チューブを挿入し細胞液で外リンパ液を還

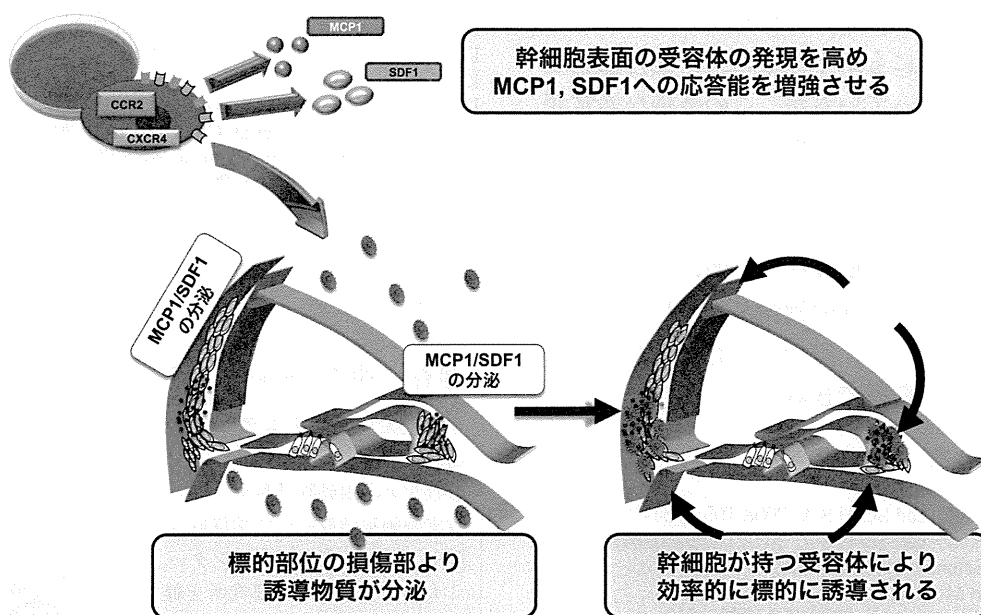

図１　幹細胞ホーミング機構を応用した内耳細胞治療法
培養シャーレ上で幹細胞（骨髄間葉系幹細胞等）にホーミング因子（MCP1, SDF1）を作用させそれらの受容体（CCR2, CXCR4）の発現を増強させる．移植前に薬物処置により蝸牛外側壁中心部にホーミング因子の発現を惹起させておき，外リンパ液中に上記前処置細胞を投与．この方法により蝸牛組織への幹細胞導入効率が大きく上昇する．

流する経半規管外リンパ液還流法を用いている(13)．同手法では手術による聴力低下はほとんど見られず，大量の細胞を外リンパ液中に導入することができるため，安全性を考慮した際の内耳細胞治療に適した投与法であると思われる．我々は細胞液環流後に骨髄間葉系幹細胞の細胞塊を半規管の小孔に挿入することにより，術後のリンパ液の漏出を防ぎ，細胞生着にも良好な結果を得ている．

8.　内耳幹細胞ホーミング機構を応用した効率的細胞誘導法の開発

実用可能な内耳幹細胞治療法の開発のためには有毛細胞やその支持細胞および内リンパ液に接する血管条細胞，蝸牛線維細胞など適切な箇所に幹細胞を導入しその微小環境（niche，ニッチ，ニッシェ）に応じて分化させることが必要である．そのためには適切な幹細胞ホーミング（標的組織へ遊走し微小環境に生着）の分子機構を理解し応用することが重要であると考えられる．

マックスプランク研究所の報告では，心筋虚血後に骨髄由来間葉系幹細胞が瘢痕層へ効率的にホーミングされるには走化性因子 MCP1，SDF1 とその受容体 CCR2，CXCR4 およびその下流において細胞遊走を制御している FROUNT による分子経路が重要な役割を担うことが明らかにされた(14)．

内耳におけるホーミングに関し，Tan らは音響障害を与えた蝸牛に多くの骨髄由来細胞が誘導され，走化性因子として SDF1 が機能していることを示している(15)．特に損傷後１週間で最も多くの骨髄由来細胞が蝸牛に誘導され，らせん靭帯の蝸牛線維細胞Ⅱ型周囲での SDF1 の発現と共に同部位への細胞誘導が示された．SDF1 が幹細胞ホーミング因子として組織損傷部への幹細胞誘導とその適応分化に関与するとの報告は多く(16)，内耳においても同因子がホーミングに重要な役割を担うと考えられる．

我々は上記のホーミング機構を応用し内耳での自然細胞誘導・修復機構を人為的に増強することにより，移植幹細胞の前処置によって MCP1，SDF1 の受容体である CCR2，CXCR4 の発現を効率的に上昇させることに成功した．同細胞を MCP1，SDF1 の発現を局所的に高めた蝸牛へ投与することにより蝸牛への幹細胞導入効率を約４倍に上昇させることが可能となった（図１）．さらに上記 Cx26 遺伝子欠損難聴モデルにおける Cx26 ギャップ結合を再構築させることに成功した（未発表）．同方法を最適化することにより大量の前駆細胞を内耳標的部位に導入し聴力回復に寄与できると考えられる．

9.　おわりに

遺伝性難聴の治療においては人工内耳の有用性も報

告されているが，本来の聴覚機能を回復させる根本的治療法は未だ存在しない．遺伝性難聴の第一次的な原因細胞は有毛細胞以外にも蝸牛線維細胞や支持細胞であることが明らかとなっているが，この多様な異常変異細胞を修復するには新たな治療戦略として多能性幹細胞を用いた効率的細胞治療法の開発が必須であると考えられる．内耳における幹細胞ホーミング機構を理解し，自然細胞誘導・修復機構を人為的に分子制御することにより，様々な多能性幹細胞を蝸牛目的部位へ導入することが可能となり，安全性と有効性の高い新規細胞治療法の開発が期待できる．

文　　献

1) Nin F, et al. Proc Natl Acad Sci U S A. 2008;105:1751-1756.
2) Nin F, et al. Proc Natl Acad Sci U S A. 2012;109:9191-9196.
3) Minowa O, et al. Science. 1999;285:1408-1411.
4) Kudo T, et al. Hum Mol Genet. 2003;12:995-1004.
5) Inoshita A, et al. Neuroscience. 2008;156:1039-1047.
6) Minekawa A, et al. Neuroscience. 2009;164:1312-1319.
7) Hoya N, et al. Neuroreport. 2004;15:1597-1600.
8) Okamoto Y, et al. Audiol Neurootol. 2005;10:220-233.
9) Kamiya K, et al. Am J Pathol. 2007;171:214-226.
10) Oshima K, et al. Cell. 2010;141:704-716.
11) Chen W, et al. Nature. 2012;490:278-282.
12) Kuroda Y, et al. Proc Natl Acad Sci U S A. 2010;107:8639-8643.
13) Iguchi F, et al. Acta Otolaryngol Suppl. 2004;43-47.
14) Belema-Bedada F, et al. Cell Stem Cell. 2008;2:566-575.
15) Tan BT, et al. J Comp Neurol. 2008;509:167-179.
16) Hattori K, et al. Blood. 2001;97:3354-3360.

著者プロフィール

神谷　和作（かみや　かずさく）

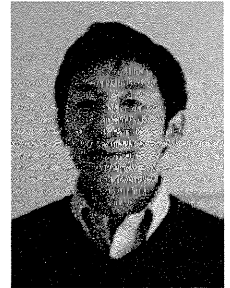

順天堂大学 医学部 耳鼻咽喉科学講座，講師，博士（獣医学）．

◇東北大応用動物学科卒，東大獣医学専攻実験動物学教室にて学位取得後，理研脳センター，東京医療センター，マイアミ大学，パスツール研究所を経て '08 年現職．◇趣味：ラグビー．◇研究テーマ：内耳幹細胞治療法の開発．